n-Butane Dehydrogenation over Vanadium Carbides: Correlating Catalytic and Electronic Properties

H. Kwon,[*,1] L. T. Thompson,[*,2] J. Eng, Jr.,[†] and J. G. Chen[‡]

*Department of Chemical Engineering, Center for Catalysis and Surface Science, University of Michigan, Ann Arbor, Michigan 48109-2136;
†Lucent Technology, Bell Laboratories, Murray Hill, New Jersey 07974; and ‡Department of Materials Science and Engineering,
Center for Catalytic Science and Technology (CCST), University of Delaware, Newark, Delaware 19716

Vanadium carbides were prepared via the temperature-programmed reaction of V_2O_5 with a CH_4/H_2 mixture and evaluated for the dehydrogenation of n-butane. Thermogravimetric analysis coupled with X-ray diffraction indicated that the solid-state reaction proceeded by the following sequential reaction: $V_2O_5 \rightarrow V_2O_3 \rightarrow V_8C_7$. The space velocity and heating rates had insignificant effects on the surface areas; however, the use of a high-temperature H_2 post-treatment caused a reduction in the surface area and carbon content. Temperature-programmed reduction results indicated that oxygen was more strongly bound to the substoichiometric vanadium carbide than to the stoichiometric material. The results were also consistent with the presence of an oxycarbide near surfaces of the passivated vanadium carbides. The passivated vanadium carbides were sufficiently activated by reduction in H_2 at 500°C for 3 h. Oxygen chemisorptive uptakes on the reduced vanadium carbides corresponded to an O/V ratio of 0.28. This oxygen-to-metal ratio is half that measured for the vanadium nitrides, suggesting that some excess carbon may have been present on surfaces of the carbides. The butane dehydrogenation turnover frequency for the vanadium carbide catalyst was $10^{-3}\ s^{-1}$ at 450°C. The corresponding turnover frequency for a Pt-Sn/Al_2O_3 catalyst was $6.3 \times 10^{-2}\ s^{-1}$. Near-edge X-ray absorption fine structure spectroscopy indicated that the vanadium carbide and nitride catalysts were partially ionic, with charge transfer being from vanadium to carbon or nitrogen. This degree of ionic bonding distinguishes the vanadium compounds from other carbides and nitrides and could partly explain their high dehydrogenation selectivities. Similarities between catalytic properties of the vanadium carbides and nitrides were likely a consequence of their similar electronic structures. The p-projected density of unoccupied states near the carbon and nitrogen K-edges nearly identical.   © 2000 Academic Press

Key Words: vanadium carbide; dehydrogenation; reduction; X-ray absorption spectroscopy.

[1] Current address: Soongsil University, Department of Chemical and Environmental Engineering, Sangdo 5-Dong, Dongjak-Ku, Seoul, Korea 156-743.

[2] To whom correspondence should be addressed. E-mail: ltt@umich.edu.

INTRODUCTION

For many years, the catalytic properties of molybdenum and tungsten carbides and nitrides have been studied. These materials catalyze a number of reactions, including hydrocarbon conversion (1–3), and their surface and adsorptive properties have been extensively characterized (4–7). Much less attention has been devoted to understanding the catalytic and sorptive properties of other carbides and nitrides. Recently vanadium carbides and nitrides have been found to be active and selective for the dehydrogenation of n-butane (8), i-butane (9), and n-hexane (10). These reactions are used to form feedstocks for the production of polymers, methyl-tert-butyl ether and substituted aromatics (11). While dehydrogenation turnover frequencies for the vanadium carbides and nitrides were much lower than those for noble metal-based catalysts, their volumetric reaction rates were comparable or superior (8, 10, 12). In addition, the early transition metals carbides and nitrides are inexpensive and tolerant to poisons (13, 14).

The goals of research described in this paper were to develop processing–structure, and structure–function, relationships for vanadium carbide catalysts. These goals were accomplished by correlating the synthesis conditions, physical and chemical properties, and n-butane dehydrogenation activities for a series of vanadium carbides. Our recent examination of several early transition metal carbides and nitrides suggested a correlation between their catalytic and solid-state bonding characteristics (8, 10). We found that the group V carbides and nitrides were very selective to alkane dehydrogenation with modest activities, while the group VI compounds were highly active with poor selectivities. A factor that we tentatively used to reconcile the results is the degree of charge transfer. For the group V carbides and nitrides, the significant difference in electronegativities would favor a high degree of charge transfer from the metal to the nonmetal atom, and therefore a very ionic bond. The converse is true for the group VI carbides and nitrides suggesting that the ability to selectively catalyze alkane dehydrogenation is influenced by the degree of ionic bonding

60

in the catalyst. In the present study, near-edge X-ray absorption fine structure (NEXAFS) was used to probe the character of bonding in the vanadium carbides (15). Analysis of the NEXAFS results was based on previous studies of carbide and nitride films on single-crystal surfaces by Chen and co-workers (9, 16–19). The vanadium carbides were also characterized using temperature-programmed reduction and oxygen chemisorption.

EXPERIMENTAL

Synthesis

The carbides were synthesized by reacting V_2O_5 powder (99.95%, 7 m^2/g, Alfa) with a mixture containing 49.9% CH_4 in H_2 (Scott) in a temperature-programmed manner. The reaction temperatures were selected on the basis of results from thermal gravimetric analysis (TGA) of the reaction of V_2O_5 and CH_4/H_2. The TGA results also provided information concerning intermediates generated during the TPR of V_2O_5 with CH_4/H_2. A Cahn Model TG-171 thermal gravimetric analyzer was used to acquire the TGA patterns starting with approximately 200 mg of V_2O_5 powder. The powder was placed in a quartz sample holder suspended in the TGA reactor.

Details concerning the reactor system that was used to synthesize the carbide catalysts are given elsewhere (20). The molar hourly space velocity, defined as the ratio of the molar flow rate of CH_4/H_2 to the moles of V_2O_5, was varied to explore its effect on the carbide microstructure. Approximately 2 g of the oxide powder were used for each run, and the gas flow rates were controlled using needle valves and measured using rotameters which were calibrated using a soap-film meter. After synthesis, the furnace was opened and the product was rapidly cooled to room temperature in the flowing CH_4/H_2 mixture, purged with He for 10 min then passivated using a mixture of 1% O_2 in He (Scott) flowing at 20 ml/min for 2 h. After passivation, the product was taken out of the reactor and stored in a desiccator for characterization and evaluation.

Characterization

Phase identification and crystallite size analysis were accomplished using a Rigaku DMAX-B X-ray diffractometer. The crystalline phases were identified by comparing the lattice parameters to those of standard compounds. The bulk carbon, nitrogen, and hydrogen contents of the materials were estimated using a Perkin–Elmer 2400 CHN analyzer equipped with an autosampler. Between 2 and 5 mg of material was placed in a Sn sample holder. After running several blanks and acetanilide standards, samples were combusted in the analyzer at 925°C in 2 atm of O_2. The effluent gases were separated using a frontal chromatographic method and the percentages of C, H, and N were recorded. The

samples were analyzed at least twice. No attempt was made to quantify the amount of oxygen in the materials.

The surface areas were measured by the BET method using a Quantasorb Model QS-17 sorption analyzer. Prior to measuring the surface areas via N_2 adsorption at −196°C, the materials were pretreated in H_2 (99.99%, Air Products) flowing at 20 cm^3/min in order to remove the passivation layer and other impurities and then purged with He. Reduction of the passivation layer was investigated via the temperature-programmed reduction of selected materials. An Altamira AMI-M catalyst characterization system equipped with thermal conductivity and mass spectrometer detectors was used to perform the temperature programmed reduction experiments. Approximately 50 mg of the catalyst was placed in a quartz U-tube over a quartz wool plug. A thermocouple was placed in the bed to ensure good thermal contact with the catalyst. The carbide bed was purged with Ar (99.998%, Cryogenic) for 10 min at room temperature, heated linearly in flowing 5.2% H_2 in Ar (Cryogenic) from room temperature to 600°C, the maximum temperature for the instrument, at 5°C/min and then held at this temperature for several hours.

Oxygen chemisorption was used to estimate the surface site densities. We prefer oxygen chemisorption over hydrogen chemisorption because hydrogen is much more prone to populate subsurface sites in carbides and nitrides (4, 10). Prior to the pulsed chemisorption measurements, the materials were pretreated using the same conditions employed prior to the surface area measurements. Calibrated volumes of 9.98% O_2 in He (Scott) were injected into the He carrier gas entering the pretreated catalyst bed. The bed was maintained at −78°C using a dry ice/acetone bath. This temperature was selected to avoid corrosive chemisorption on the carbides and nitrides (4, 10). Oxygen that was not adsorbed was detected and recorded. When the O_2 pulses reached a constant area, the surface was considered to be saturated. The amount of oxygen adsorbed was calculated from the peak areas. The BET surface area and O_2 uptake measurements were replicated, and the reported values are averages.

The NEXAFS experiments were performed on the Exxon U1A beamline at the National Synchrotron Light Source, Brookhaven National Laboratory. The NEXAFS spectra were recorded near the L-edge of V and the K-edges of C, N, and O, by measuring the electron-yield intensity using a channeltron electron multiplier located near the sample holder. To make the electron-yield method more sensitive to the surface region of the samples, the front of the channeltron was biased by a retarding voltage of −100 eV to repel low-energy, secondary electrons (15). The NEXAFS spectra were normalized to have the same step-height to eliminate possible concentration effects between different samples. The carbide and nitride powders were pressed into a stainless steel sample holder of ~10 mm in diameter
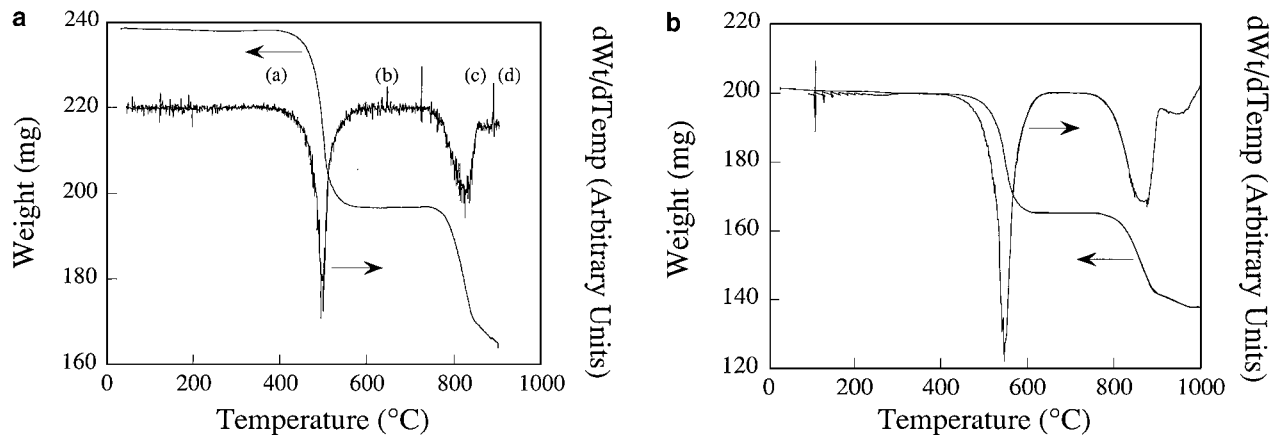
FIG. 1. Thermal gravimetric analysis of the reaction of V_2O_5 with an equimolar mixture of CH_4 and H_2 using heating rates of (a) $60°C/h$ and (a) $180°C/h$.

and ~1 mm in depth, as described previously (21). The powder samples were heated by resistively heating two tungsten wires (0.025 cm in diameter) spot-welded onto the sample holder. The sample temperature was measured by a chromel–alumel thermocouple. The samples were pretreated in 20 Torr of H_2 at $450°C$ for 0.5 h. This type of pretreatment was previously found to remove most of the oxygen from carbides and nitrides (22, 23). The NEXAFS spectra were recorded after the reaction chamber was evacuated to below 10^{-8} Torr.

Catalytic Properties

The catalytic properties were measured using a 6 mm OD quartz U-tube flow reactor. The catalyst was loaded into the reactor on top of a plug of quartz wool and reduced in H_2 (99.99%, Air Products). A chromel–alumel thermocouple was inserted directly into the catalyst bed to ensure accurate temperature control. After reduction in H_2, the bed was cooled to $450°C$ and the reactant mixture flow was initiated. The reaction rates were measured at temperatures between 375 and $450°C$, and atmospheric pressure. The reactant mixture consisted of 4% C_4H_{10}, 60% H_2, and 36% He, and the flow rate was held constant at 50 ml/min. The reactor loading was adjusted to limit the butane conversion to 2% at $450°C$ so that the system could be treated as a differential reactor. The equilibrium conversion to butenes and butadienes is ~13% at $450°C$. The reaction products were separated using a 3.05 m *n*-octane/Porasil C packed column (Alltech Associates) and analyzed using an HP 5890 gas chromatograph with a flame ionization detector. Other details concerning the reactor and flow system can be found elsewhere (20).

RESULTS AND DISCUSSION

Vanadium Carbide Synthesis

The known vanadium carbide phases are VC, V_8C_7, V_4C_3, θ-$V_4C_{2.67}$, and V_2C. Thermal gravimetric analysis (TGA)

patterns for the reaction of V_2O_5 with CH_4/H_2 flowing at a rate of 50 ml/min (corresponds to space velocity of 60 h^{-1}) are illustrated in Fig. 1. There appeared to be two major reaction or desorption events. The first event commenced at ~$400°C$ and produced a peak in the derivative plot at ~$490°C$ when a heating rate of $60°C/h$ was employed. The weight loss associated with this event (17.3 and 17.4% at heating rates of 60 and $180°C/h$, respectively) was consistent with the conversion of V_2O_5 to V_2O_3. The second event occurred over a relatively broad temperature range (750–$900°C$). The total weight loss up to $1000°C$ (31.2 and 31.1% at heating rates of 60 and $180°C/h$, respectively) was very close to the theoretical value for the conversion of V_2O_5 to V_8C_7. The transformation temperatures shifted to higher temperatures when higher heating rates were employed. This type of behavior is typically a consequence of the rate-limiting process being diffusion of species into and/or out of the solid, although surface reaction or desorption processes cannot be ruled out. Diffraction patterns for solids isolated by quenching the reaction at various temperatures are shown in Fig. 2. All of the samples were passivated by slowly leaking air into the TGA reactor prior to removal from the system. The only crystalline reaction intermediate was V_2O_3 as indicated in Table 1. The apparent solid state

TABLE 1

Weight Loss During the Carburization of V_2O_5 with a CH_4/H_2 Mixture^a

Sampling point	a	b	c	d
Temperature (°C)	400	650	850	910
Crystalline phase by XRD	V_2O_5	V_2O_3	V_8C_7, V_2O_3	V_8C_7
Theoretical density (g/cm^3)	3.36	5.02	–	5.64
Actual weight loss (%)	0	17.3	–	31.2
Theoretical weight loss (%)	0	17.6	–	32.4

^{a} The heating rate for the corresponding thermal gravimetric analysis experiments was $60°C/h$.
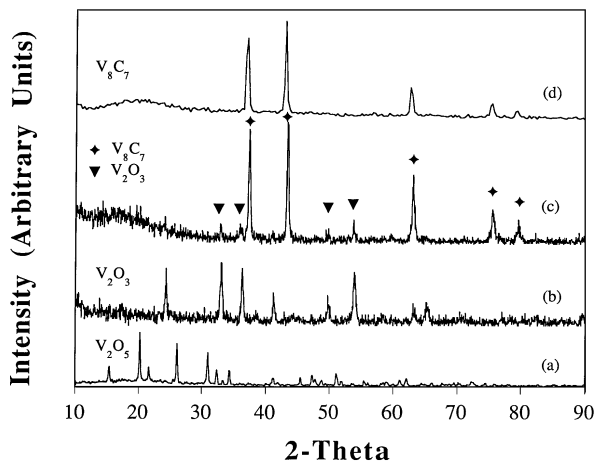
FIG. 2. X-ray diffraction patterns of products from the reaction of V_2O_5 and NH_3. These materials were collected after quenching the reaction at (a) 400, (b) 650, (c) 850, and (d) 910°C. The heating rate was 60°C/h.

reaction pathway of $V_2O_5 \rightarrow V_2O_3 \rightarrow V_8C_7$ is consistent with reports by Kapoor and Oyama (24) who used product gas analysis and X-ray diffraction to track development of the carbide.

To study affects of the synthesis parameters on the carbide microstructural properties, the space velocity and heating rate were varied. In addition effects of the soak time and hydrogen post-treatment were investigated. The hydrogen post-treatment involved holding the solid product in flowing hydrogen (150 cc/min) at the final reaction temperature for an hour. The vanadium carbides were prepared using a final temperature of 910°C. Table 2 summarizes the results. Varying the space velocity and heating rate, within the ranges explored, did not significantly affect properties of the carbides. In particular, the surface area varied by less than 20% on varying the space velocity. The effect of the H_2 post-treatment on the surface area was, however, clear and significant. The carbide prepared using the H_2 post-treatment step had a much lower surface

area than the material prepared without the treatment. The H_2 post-treatment also resulted in a substantial reduction in the carbon content. The H_2 post-treated carbide contained 16.0 wt% carbon while the untreated material contained 17.8% carbon. Stoichiometric V_8C_7 contains 17.1% carbon, suggesting that the H_2 post-treated carbide was carbon deficient and the untreated material contained a small amount of excess carbon. It is important to note that interstitial carbides like V_8C_7 are typically stable over a broad range of composition and only rarely are stoichiometric (25).

The apparent carbon deficiency observed for the passivated, H_2 post-treated carbide could be a consequence of the presence of oxygen in the lattice. Like carbon and nitrogen, oxygen can occupy octahedral interstitial sites in the lattice (26). While the amount of oxygen was not quantified, its presence in the passivated vanadium carbides was evident from the TPR and NEXAFS results. There are other explanations for the carbon deficiency. Vanadium metal may have been produced during H_2 post-treatment. If V_8C_7 and vanadium metal were the only phases present, the metal would account for more than 6 wt% of the sample and should produce a diffraction pattern. No peaks attributable to vanadium metal were detected in the X-ray diffraction patterns, although it is possible that the metal was amorphous. It is also possible that lower stoichiometry vanadium carbides were present in the H_2 post-treated material. Phases including θ-$V_4C_{2.67}$ (13.6%) and V_2C (10.5%) have tentatively been ruled out on the basis of the absence of evidence in the X-ray diffraction patterns. We cannot, however, rule out the presence of V_4C_3 (15 wt% carbon). The lattice structure of V_4C_3 is very similar to that of V_8C_7, and their diffraction patterns are nearly identical.

Excess carbon in the untreated carbide was likely graphitic and/or polymeric. We ruled out the presence of high-stoichiometry carbide phases like VC (19.1 wt%). If only V_8C_7 and VC were present, VC would account for ~35 wt% of the material and should produce strong peaks in the diffraction pattern. The excess carbon was equivalent to about 2 monolayers assuming that 10^{19} atoms are required to cover 1 m^2 of surface (or ~2 mg/m^2).

Temperature-Programmed Reduction

Passivation with O_2 introduces oxygen into the carbide or nitride surface and renders the material inactive (4, 12, 13). Prior to measurement of the adsorptive and catalytic properties, oxygen in the passivation layer is typically removed by H_2 reduction. The appropriate conditions for reduction of the vanadium carbides were defined on the basis of the temperature-programmed reduction results.

Temperature-programmed reduction spectra for selected H_2 post-treated (VC-4) and untreated (VC-5) vanadium carbides are illustrated in Fig. 3a and b, respectively. Much of the signal attributed to CO ($m/e = 28$) was part of the
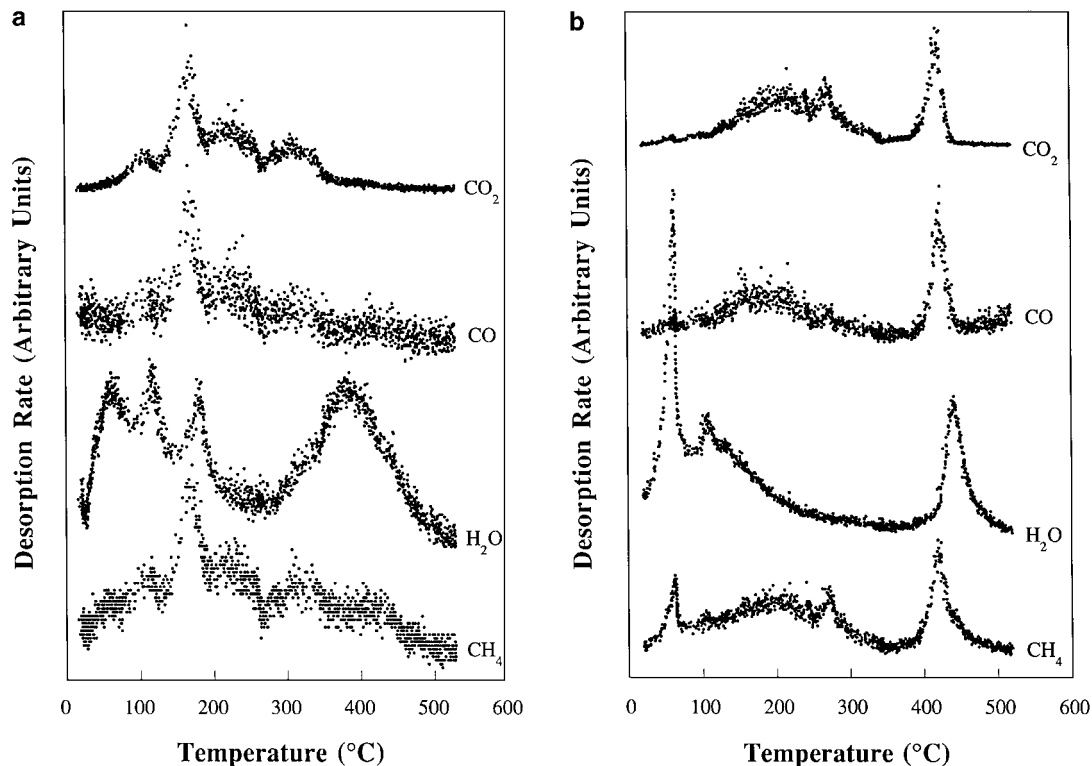
TABLE 2

Synthesis Parameters and Surface Areas for the Vanadium Carbides

Catalyst	Space velocity (h^{-1})	Heating rate (°C/h)	Soak time[a] (h)	H_2 treatment time (h)	Surface area (m^2/g)
VC-1	40	60	1	1	9.1
VC-2	40	180	1	1	8.2
VC-3	80	60	1	1	10
VC-4	80	180	1	1	12
VC-5	80	180	1	0	19
VC-6	80	180	0	1	10

[a] The soak and H_2 treatment temperatures were 910°C.

FIG. 3. Species produced during the temperature programmed reduction of (a) VC-4 and (b) VC-5 with a mixture of 5.2% H_2 in Ar. The heating rate was 5°C/min.

fragmentation pattern for CO_2 ($m/e = 44$). Following the desorption of physisorbed H_2O ($m/e = 18$) at ~200°C, additional amounts of H_2O were produced at higher temperatures. Water that desorbed at high temperatures was coincident with the consumption of H_2 (see Fig. 4). This observation suggested that H_2O produced at temperatures in excess of 350°C was due to the reduction of oxygen in the passivation layer. Carbon was also removed from the surface in the form of CH_4, CO_2, and perhaps CO. Given the relatively low temperatures, we believe carbon in the CH_4 product was a part of the carbide lattice (carbidic). The hydrogenation of graphitic carbon typically requires much higher temperatures (27). The formation of CO_2 suggests that carbon and oxygen in the passivation layer were able to react. We took this as evidence of an oxycarbide at the surface since the reaction of vanadium oxide with carbon is not favored at the temperatures where CO_2 desorbed. The carbothermal reduction of V_2O_5 would require temperatures near 660°C (28).

While species produced during TPR of the H_2 posttreated and untreated carbides were similar, they desorbed from the H_2 post-treated carbides at substantially higher temperatures. This is consistent with the H_2 post-treated carbides being carbon deficient. A carbon-deficient carbide would more strongly bind carbon and oxygen than a carbide containing excess carbon. The temperature for H_2O
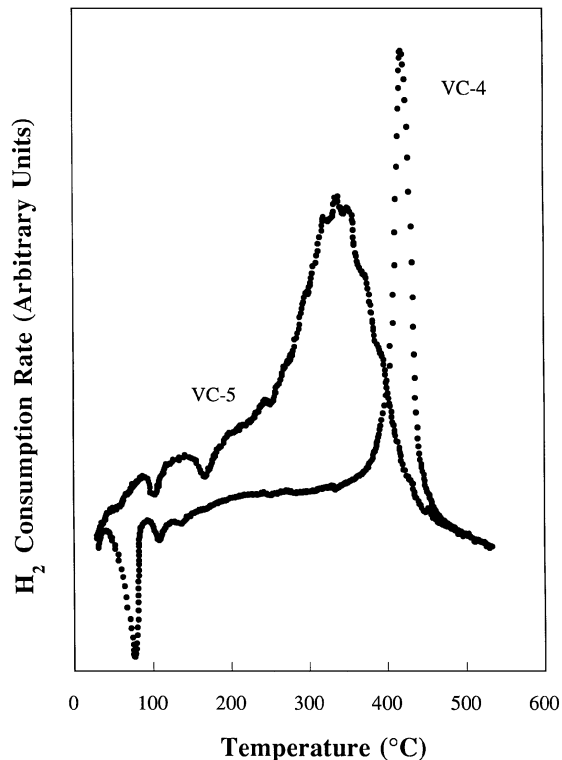

FIG. 4. Hydrogen consumption rate during the temperature programmed reduction of VC-4 and VC-5 with a mixture of 5.2% H_2 in Ar. The heating rate was 5°C/min.

desorption from the H_2 post-treated carbide (~440°C) was slightly lower than that for the vanadium nitride (~480°C) (12). This result provides insight into the influence of the nonmetal atom on the surface and electronic properties of the carbides and nitrides. Apparently oxygen was more strongly bound by the vanadium nitride than the carbide. This is consistent with vanadium in the nitride being more oxidized than vanadium in the carbide. The degree of oxidation was further investigated using NEXAFS.

Catalytic Properties

The reaction rates and product selectivities were measured after reducing the vanadium carbides at 500°C in H_2 for 3 h. This treatment was selected on the basis of the TPR results and appeared to be sufficient to remove the passivation layer. The untreated vanadium carbide (VC-5) was essentially inactive under the conditions employed in this research. This result is consistent with the surface being substantially blocked by graphitic and/or polymeric carbon. Reaction rates for a H_2 post-treated vanadium carbide (VC-4) are given in Table 3. For comparison, butane conversion rates for the VN (14 m²/g), Mo_2C (62 m²/g), and Pt-Sn/Al_2O_3 (0.3% Pt, 1.2% Sn, and 1.8% Na) catalysts are included. The Pt-Sn/Al_2O_3 catalyst was optimized for dehydrogenation (29). The VN catalyst was reduced in H_2 for 3 h at 500°C, and the Mo_2C and Pt-Sn/Al_2O_3 catalysts were pretreated in H_2 for 3 h at 480°C. No significant changes in the reaction rates were observed when the materials were ground or the flow rate increased, which indicated the absence of external transport limitations. The reaction rates reached steady-state after approximately 1 h on stream and were reproducible to within ±10% during subsequent runs.

Steady-state reaction rates for the H_2 post-treated vanadium carbide were comparable to those for the vanadium nitride but lower than those for the Mo_2C and Pt-Sn/Al_2O_3 catalysts. The vanadium carbide possessed excellent selec-
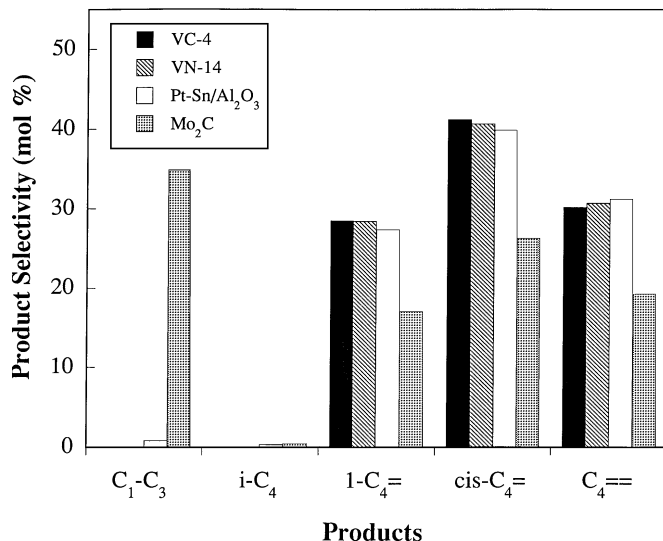

FIG. 5. Butane conversion selectivities measured at 450°C and 101 kPa. The abbreviations C_1–C_3, i-C_4, 1-C_4=, cis-C_4=, and C_4== represent hydrocarbons containing 1 to 3 carbon atoms, i-C_4H_{10}, 1-C_4H_8, cis-2-C_4H_8, and 1,3-C_4H_6, respectively.

tivities toward dehydrogenation products (Fig. 5). The butane dehydrogenation selectivities were greater than 98%. The vanadium carbide produced almost the same product distribution as the vanadium nitride and Pt-Sn/Al_2O_3 catalysts. Note that the selectivities were determined at similar conversions.

Oxygen chemisorption was used to normalize the reaction rates and qualitatively assess the degree of coverage by excess carbon. The H_2 post-treated and untreated carbides were reduced in H_2 at 500°C for 3 h prior to the chemisorption measurements. The O_2 uptake for the H_2 post-treated carbide was 28 μmol O_2/g. This corresponds to a site density of 1.4×10^{14} O_2/cm². Oxygen chemisorbs dissociatively on vanadium carbide surfaces (30), therefore the oxygen uptake also corresponds to an O/V ratio of 0.28 assuming that the surface metal atom density for V_8C_7 is 10^{15} V/cm². For comparison the vanadium nitride chemisorbed 45 μmol O_2/g corresponding to an O/V ratio of 0.56 (12). Given the similar structural and electronic properties of V_8C_7 and VN, the difference suggests that about half of the carbide surface may not have been accessed during oxygen chemisorption. Nevertheless, the O/V ratio for the H_2 post-treated vanadium carbide was similar to O/Mo ratios that were observed for α-Mo_2C (31) and γ-Mo_2N (4) (0.13 and 0.21, respectively). The O_2 uptake for the untreated vanadium carbide was less than the detection limit, again suggesting that surface sites were blocked by excess carbon. The Mo_2C and Pt-Sn/Al_2O_3 catalysts chemisorbed 50 and 2.8 μmol O_2/g, respectively, after reduction in H_2 for 3 h at 480°C. Oxygen did not chemisorb to the Al_2O_3, indicating that oxygen uptake for the

TABLE 3

Butane Conversion Rates for the Vanadium Carbides and Several Reference Catalysts[a]

Catalyst	Gravimetric reaction rates (nmol/g · s)	Volumetric reaction rates (nmol/cm³ · s)	Turnover frequency[b] (s⁻¹ × 10³)	Apparent activation energy (kcal/mol)
VC-4	54	152	1.0	41
VN	89	67	1.0	37
Mo_2C	2014	8962	20	23
Pt-Sn/Al_2O_3	354	690	63	28

[a] Measured under differential conditions at 450°C and 101 kPa for a reactant containing 4% C_4H_{10}, 60% H_2, and 36% He. The catalysts were reduced in H_2 for 3 h at 480–500°C.
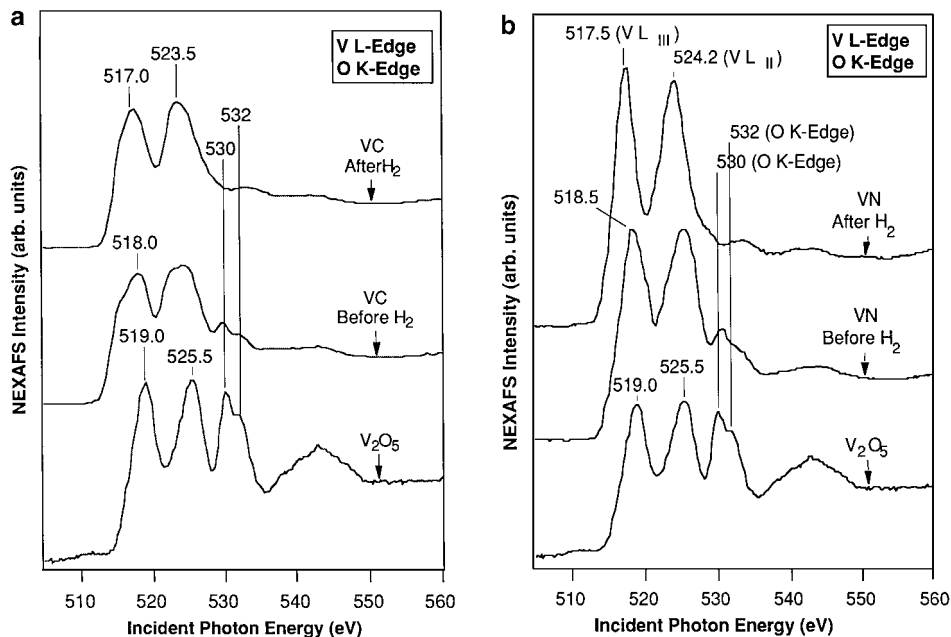
[b] Based on oxygen chemisorption at −78°C.

FIG. 6. Near-edge X-ray absorption fine structure spectra at the V L-edge and O K-edge for the (a) vanadium carbide and (b) nitride catalysts, before and after H_2 treatment.

Pt-Sn/Al$_2$O$_3$ catalyst was associated with the Pt and/or Sn. The O/Pt ratio of 0.36 for this catalyst was very close to values reported elsewhere for supported Pt-Sn catalysts (32).

Turnover frequencies determined on the basis of the oxygen uptake allow a more direct comparison of intrinsic properties of the V$_8$C$_7$, VN, and Pt-based catalysts. Turnover frequencies for the V$_8$C$_7$ catalyst were equal to those for the VN catalyst but more than an order of magnitude lower than those for the Pt-Sn/Al$_2$O$_3$ catalyst. The turnover frequency for the Pt-Sn/Al$_2$O$_3$ catalyst should be considered a lower limit because oxygen chemisorbs onto Pt and Sn although Pt is the principal catalytic species (32). If we assume a conservative dispersion of 50% for Pt in this catalyst, the turnover frequency would be 0.043 s^{-1} at 450°C. Turnover frequencies for the V$_8$C$_7$ and VN catalysts were also much lower than those for the Mo$_2$C catalyst.

Given the similar sizes and electronic properties of carbon and nitrogen, similarities between the catalytic properties of carbides and nitrides with identical structures are not unexpected. On the other hand, early transition metal nitrides can be converted into the carbides by the topotactic substitution of carbon for nitrogen (26, 33). Butane is a better carburizing agent than methane and the vanadium nitride could be carburized during the butane conversion experiments. X-ray diffraction patterns for the used nitrides were, however, nearly identical to those for the fresh materials, indicating that the nitrides did not transform into bulk carbides. If carburization occurred, it probably was restricted to the surface.

Apparent activation energies for the vanadium carbides and nitrides were similar, which is consistent with these ma-

terials sharing the same reaction mechanism (see Table 3). The V$_8$C$_7$ and VN catalysts had higher activation energies than the Mo$_2$C and Pt-Sn/Al$_2$O$_3$ catalysts. This result indicates that kinetics of the elementary reactions or reaction mechanisms for the vanadium carbide and nitride catalysts were different from those for the molybdenum carbide and Pt-based catalysts.

Near Edge X-Ray Absorption Fine Structure

Figure 6 shows the vanadium L-edge and oxygen K-edge features of the H$_2$ post-treated vanadium carbide before and after pretreatment in H$_2$. For comparison, V L-edge spectra for the VN catalyst and V$_2$O$_5$ powder are also included. The NEXAFS spectra in this energy range can be divided into two regions: peaks observed at energies below 530 eV are related to the V L$_{III}$ and L$_{II}$ near-edge features, and the peak positions are related to the vanadium oxidation state (15, 34). The near-edge peaks at energies above 530 eV are associated with the oxygen K-edge features, which are due to the electronic transition of O 1s electrons to several partially-filled and unfilled molecular orbitals of vanadium oxides or oxycarbides (15, 34).

The detection of oxygen near-edge features indicated the presence of oxygen in the passivated carbides and nitrides. Most of the oxygen was readily removed by heating the material in H$_2$ (20 Torr, 450°C, 0.5 h), as indicated by the significant reduction of the intensities of the O K-edge features after H$_2$ pretreatment. However, the results show that a relatively weak O K-edge feature at ~534 eV remains after the H$_2$ treatment, suggesting the presence of a small amount of oxygen in the vanadium carbide and nitride. From a

previous NEXAFS study of the adsorption of oxygen on a V(110) single-crystal surface (35), the relative intensity ratio of the V L-edge and O K-edge features can be used to estimate the amount of oxygen. On the basis of the intensity ratios in Fig. 6, we estimated that the atomic ratio of oxygen to vanadium is less than 15% after the H_2 treatment. It is not presently clear how much oxygen, if any, remained in the carbides and nitrides following reduction in H_2 at 500°C and atmospheric pressure for 3 h.

Peak positions of the L_{III} and L_{II} features shifted to lower energies after the H_2 treatment. As shown in Fig. 7, there is a nearly linear relationship between the vanadium oxidation state and the NEXAFS peak positions. Utilizing this relationship, average oxidation states for vanadium in surfaces of the passivated vanadium carbide and nitride catalysts were predicted to be approximately +4. This result is consistent with the presence of an oxycarbide or oxynitride at the surface. Average oxidation states for vanadium in the reduced vanadium carbide and nitride catalysts were +1.9 and +2.7, respectively. Apparently a substantial amount of charge is transferred from vanadium to the nonmetal atoms in these materials. It is important to note that the oxidation state of the reduced vanadium carbide powder was slightly higher than that of vanadium carbide films produced from a V(110) single-crystal surface (+1.2). This observation is consistent with the presence of oxygen in the vanadium carbide powder, which should result in an increase in the average vanadium oxidation state.
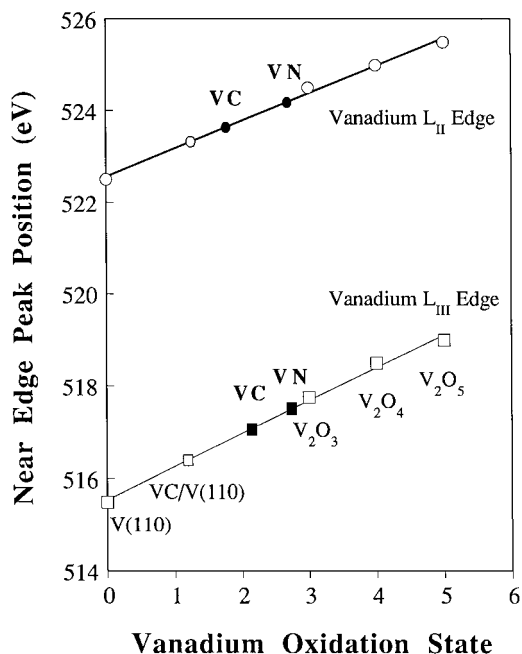

FIG. 8. Near-edge X-ray absorption fine structure spectra at the C and N K-edges for the (a) vanadium carbide and (b) nitride catalysts after H_2 treatment.

The C or N K-edge NEXAFS spectra are related to the p-projected density of unoccupied states in carbides or nitrides (15). Results for the reduced vanadium carbides and nitrides are summarized in Fig. 8. For ease of comparison, peak positions of the t_{2g} features were aligned to the same relative energy (0 eV). The K-edge features of vanadium carbide and nitride were very similar: both are characterized by two relatively sharp t_{2g} and e_g features that appeared at the same relative energies, and both have a relatively intense and broad $3a_{1g} + 4t_{1u}$ feature.

The most important conclusion from the NEXAFS results is that the vanadium carbide and nitride catalysts can be characterized as partially ionic compounds, as indicated by the significant degree of electronic charge transfer from vanadium to carbon or nitrogen. In previous surface science studies Chen and co-workers (17) found that bonding in molybdenum carbide films on Mo(110) crystals was essentially covalent with little charge transfer between molybdenum and carbon. Considering that vanadium carbide films on V(110) crystals were more active than the molybdenum carbide films in activating C–H bonds, it was proposed that the degree of ionic bonding in carbides or nitrides was related to their ability to activate C–H bonds (17, 18). The strong degree of ionic bonding and excellent dehydrogenation activities of V_8C_7 and VN catalysts described in this paper provide additional experimental support regarding such relationships.

FIG. 7. Correlation between the near-edge peak position and the formal oxidation states of vanadium in various compounds. This correlation was used to estimate oxidation states for vanadium in the carbide and nitride catalysts.
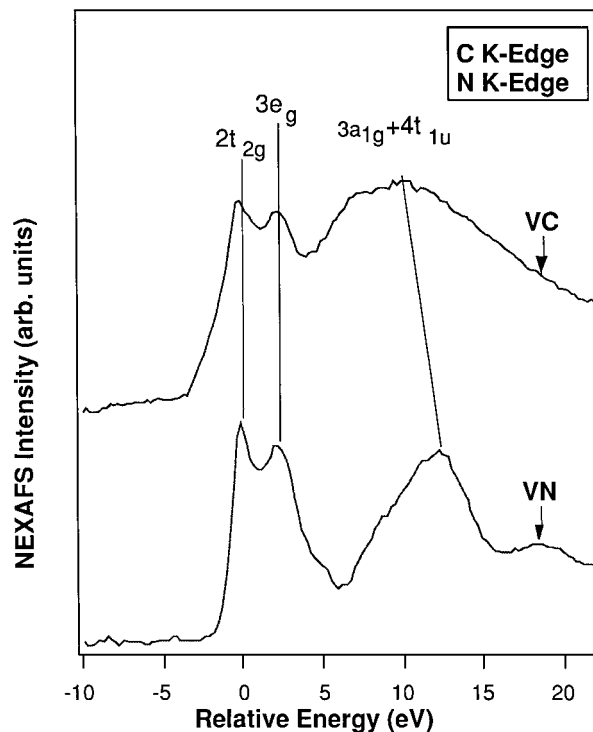
SUMMARY

Thermal gravimetric analysis and X-ray diffraction were used to determine solid-state reaction pathways and define conditions for the production of stoichiometric vanadium carbides. The reaction of V_2O_5 with an equimolar mixture of CH_4 and H_2 produced V_2O_3 then V_8C_7. Of the synthesis parameters that were varied, only the H_2 post-treatment step significantly influenced properties of the vanadium carbides. The H_2 post-treated vanadium carbide had a lower surface area and C:V ratio than the untreated material. Water, CO, CO_2, and CH_4 were produced during temperature-programmed reduction of the passivated vanadium carbides. These species desorbed from the H_2 post-treated carbides at substantially higher temperatures than from the untreated materials. This observation is consistent with the H_2 post-treated materials being carbon deficient. The TPR and NEXAFS results suggested that an oxycarbide was present at surfaces of the passivated carbides. These results also indicated that pretreatment in H_2 at 500°C for 3 h was sufficient to reduce the passivation layer. The O_2 uptake for the H_2 post-treated carbide was 28 μmol O_2/g corresponding to a site density of 2.8×10^{14} O/cm^2. Oxygen did not chemisorb to the untreated vanadium carbide, suggesting that the surface sites were blocked by excess carbon.

Turnover frequencies for the V_8C_7 catalysts were nearly identical to those for the VN catalysts but more than an order of magnitude lower than those for the Mo_2C and Pt-Sn/Al_2O_3 catalysts. However, dehydrogenation selectivities for the vanadium carbide and nitride catalysts were very similar to those for the Pt-Sn/Al_2O_3 catalyst. Electronic properties of vanadium carbides, as accessed using NEXAFS, were similar to those for the vanadium nitride. There was a substantial amount of charge transfer from vanadium to the nonmetal atom as indicated by the average oxidation states (+1.9 and +2.7 for V_8C_7 and VN, respectively). In comparison, bonding in group VI carbides and nitrides does not appear to result in a significant degree of charge transfer between the metal and nonmetal atoms. We have concluded that the ability to selectively catalyze butane dehydrogenation was at least partly due to the ionic bonding present in the V_8C_7 and VN catalysts.

ACKNOWLEDGMENTS

REFERENCES

1. Levy, R. B., and Boudart, M., *Science* **181**, 547 (1973).

2. Leclercq, L., Imura, K., Yoshida, S., Barbee, T., and Boudart, M., *in* "Preparation of Catalysts II" (B. Delmon, Ed.), p. 627. Elsevier, New York, 1978.

3. Ribeiro, F. H., Dalla Betta, R. A., Guskey, G. J., and Boudart, M., *Chem. Mater.* **3**, 805 (1991).

4. Choi, J., Brenner, J. R., Colling, C. W., Demczyk, B. G., Dunning, J., and Thompson, L. T., *Catal. Today* **15**, 201 (1992).

5. Oyama, S. T., *Catal. Today* **15**(2), 179 (1992).

6. Gubanov, V. A., Ivanovsky, A. L., and Zhukov, V. P., "Electronic Structure of Refractory Carbides and Nitrides." Cambridge Univ. Press, Cambridge, MA, 1994.

7. Choi, J.-G., Lee, H. J., and Thompson, L. T., *Appl. Surf. Sci.* **78**, 299 (1994).

8. Neylon, M. K., Choi, S., Kwon, H., Curry, K. E., and Thompson, L. T., *Appl. Catal. A* **183**, 253 (1999).

9. Chen, J. G., Fruhberger, B., Weisel, M. D., Baumgartner, J. E., and DeVries, B. D., *in* "The Chemistry of Transition Metal Carbides and Nitrides" (S. T. Oyama, Ed.). Blackie Academia and Professional, Glasgow, 1996.

10. Neylon, M. K., Bennett, C., Waldecker, J., and Thompson, L. T., *Appl. Catal. A*, submitted for publication (1999).

11. Buonomo, R., Sanfilippo, D., and Trifiro, F., *in* "Handbook of Heterogeneous Catalysis" (G. Ertl, H. Knözinger, and J. Weitkamp, Eds.), p. 2140. Wiley-VCH, Weinheim, Germany, 1997.

12. Kwon, H., Choi, S., and Thompson, L. T., *J. Catal.* **183**, 000 (1999).

13. Markel, E. J., and Van Zee, J. W., *J. Catal.* **126**, 643 (1990).

14. Dhandapani, B., Ramanathan, S., Yu, C. C., Fruhberger, B., Chen, J. G., and Oyama, S. T., *J. Catal.* **176**, 61 (1998).

15. Chen, J. G., *Surf. Sci. Rep.* **30**, 1 (1997).

16. Chen, J. G., *J. Catal.* **154**, 80 (1995).

17. Chen, J. G., *Chem. Rev.* **96**, 1477 (1996).

18. Chen, J. G., Fruhberger, B., Eng, J., and Bent, B. E., *J. Mol. Catal. A* **131**, 285 (1998).

19. Chen, J. G., Eng, J., and Kelty, S. P., *Catal. Today* **43**, 147 (1998).

20. Kwon, H., Ph.D. Dissertation, University of Michigan, 1998.

21. Chen, J. G., DeVries, B. D., Lewandowski, J. T., and Hall, R. B., *Catal. Lett.* **23**, 25 (1994).

22. Kapoor, R., Oyama, S. T., Fruhberger, B., DeVries, B. D., and Chen, J. G., *Catal. Lett.* **34**, 179 (1995).

23. Kapoor, R., Oyama, S. T., Fruhberger, B., and Chen, J. G., *J. Phys. Chem. B* **101**, 1543 (1997).

24. Kapoor, R., and Oyama, S. T., *J. Solid State Chem.* **120**, 320 (1995).

25. Pierson, H. O. "Handbook of Refractory Carbides and Nitrides: Properties, Characteristics, Processing and Applications." Noyes Publications, Westwood, NJ, 1996.

26. Toth, L. E., "Transition Metal Carbides and Nitrides." Academic Press, New York, 1971.

27. McCarty, J. G., and Wise, H., *J. Catal.* **57**, 406 (1979).

28. Weimer, A. W., *in* "Carbide, Nitride and Boride Materials Synthesis and Processing" (A. W. Weimer, Ed.). Chapman and Hall, NY, 1997.

29. Pt-Sn/Al_2O_3 catalyst was provided by the Amoco Oil Company.

30. Frantz, P., and Didziulis, S. V., *Surf. Sci.* **412/413**, 384 (1998).

31. Choi, J., Brenner, J. R., and Thompson, L. T., *J. Catal.* **154**, 33 (1995).

32. Balakrishnah, K., and Schwank, J., *J. Catal.* **127**, 287 (1991).

33. Volpe, L., and Boudart, M., *J. Solid State Chem.* **59**, 348 (1985).

34. Chen, J. G., Kim, C. M., Fruhberger, B., DeVries, B. D., and Touvelle, M. S., *Surf. Sci.* **321**, 145 (1994).

35. Kim, C. M., Fruhberger, B., DeVries, B. D., and Chen, J. G., *Surf. Sci.* **327**, 81 (1995).